NASA Technical Memorandum 83600

Coaxial Carbon Plasma Gun Deposition of Amorphous Carbon Films

Daniel M. Sater, Daniel A. Gulino,
and Sharon K. Rutledge
Lewis Research Center
Cleveland, Ohio

March 1984

NASA

47 1 1 RN/NASA-TM-83600

DISPLAY 47/2/1

84N20404*# ISSUE 10 PAGE 1587 CATEGORY 76 RPT#: NASA-TM-83600

E-2012 NAS 1.15:83600 84/03/00 20 PAGES UNCLASSIFIED DOCUMENT

UTTL: Coaxial carbon plasma gun deposition of amorphous carbon films

AUTH: A/SATER, D. M.; B/GULINO, D. A.; C/RUTLEDGE, S. K. PAA: A/(Cincinnati Univ.); C/(Cleveland State Univ.)

CORP: National Aeronautics and Space Administration. Lewis Research Center, Cleveland, Ohio. AVAIL.NTIS SAP: HC A02/MF A01

MAJS: /*CARBON/*COAXIAL PLASMA ACCELERATORS/*PLASMA GUNS/*THIN FILMS

MINS: / ELECTRICAL RESISTIVITY/ ELECTRON MICROSCOPY/ SPECTRUM ANALYSIS/ SYSTEM EFFECTIVENESS/ X RAY DIFFRACTION

ABA: Author

ABS: A unique plasma gun employing coaxial carbon electrodes was used in an attempt to deposit thin films of amorphous diamond-like carbon. A number

COAXIAL CARBON PLASMA GUN DEPOSITION OF AMORPHOUS CARBON FILMS

Daniel M. Sater[1], Daniel A. Gulino, and Sharon K. Rutledge[2]

National Aeronautics and Space Administration
Lewis Research Center
Cleveland, Ohio 44135

E-2012

SUMMARY

A unique plasma gun employing coaxial carbon electrodes has been used in an attempt to deposit thin films of amorphous "diamond-like" carbon. A number of different structural, compositional, and electrical characterization techniques were used to characterize these films. These included scanning electron microscopy, scanning transmission electron microscopy, X-ray diffraction and absorption, spectrographic analysis, energy dispersive spectroscopy, and selected area electron diffraction. Optical absorption and electrical resistivity measurements were also performed. The films were determined to be primarily amorphous, with poor adhesion to fused silica substrates. Many inclusions of particulates were found to be present as well. Analysis of these particulates revealed the presence of trace impurities, such as Fe and Cu, which were also found in the graphite electrode material. Hence it was concluded that the electrodes were the source of these impurities. No evidence of diamond-like crystallite structure was found in any of the film samples. Details of the apparatus, experimental procedure, and film characteristics are presented in this paper.

INTRODUCTION

The consistent preparation of carbon films possessing diamond-like properties has been a goal sought after by many researchers in the past decade. Such films may be hard, transparent, chemically inert, electrically insulating, and have been reported to range from amorphous to polycrystalline in structure. Thus they would find wide use in a number of aerospace applications, including insulating gates for semiconductor devices, protective coatings for surfaces, AR coatings for solar cells, etc.

In 1971 Aisenberg and Chabot (ref. 1) reported the first successful deposition of diamond-like carbon films using an ion beam technique. Since then, a number of other methods have been used to deposit such films, including ion beam sputtering of a carbon target (ref. 2) and hydrocarbon cracking in a dc or rf glow discharge (refs. 3 and 4). In the work to be reported here, a coaxial carbon plasma railgun has been used to deposit carbon films on fused silica substrates in an effort to produce diamond-like films.

Briefly, the concept of railgun operation is as follows: an electric current traveling in a circular path gives rise to a perpendicular magnetic field which in turn interacts with the current to create a Lorentz force. This force accelerates the projectile (in this case, a carbon plasma) along the rails and out of the gun. The behavior of plasma railguns has been investigated previously (refs. 5 to 9), and some work has been performed using

[1]University of Cincinnati, Cincinnati, Ohio.
[2]Cleveland State University, Cleveland, Ohio.

pulsed plasma guns for diamond-like film preparation (refs. 10 and 11). In that work, the source of carbon was that resulting from plasma dissociation of organic gases such as methane, and polycrystalline films were reported. In the present work, the same plasma gun concept was used with the gun modified to employ carbon electrodes, In this way, films could be deposited from a nearly 100 percent carbon plasma with a provision for introducing hydrogen separately, if desired, rather than bringing it in continuously as a constituent of the plasma carrier gas (although this aspect of the operation was not a part of the present work). If films could be produced in this way, the high thermal conductivity of polycrystalline carbon would make it ideal as a heat spreading film for a variety of electronics applications. A schematic drawing of the apparatus is presented in figure 1.

APPARATUS AND PROCEDURE

Coaxial Plasma Gun Mechanism

The plasma gun consisted of two coaxial carbon electrodes made of spectroscopic grade graphite (see figs. 2 and 3). The outer (negative) electrode was a hollow cylinder with a larger inside diameter along one half of its length and a smaller inside diameter along the other half. A tapered portion connected the two (see fig. 2). The inner (positive) electrode was a carbon rod of similar shape, supported by a polytetrafluoroethylene (Teflon®) cylinder which centered it within the outer electrode and allowed it to slide axially. Stainless steel reinforcing rods were embedded in the inner electrode for added strength; otherwise the electrode regularly cracked.

To fire the gun, the inner electrode was drawn forward by two solenoids until the two tapered surfaces came into contact. The current, fed into the system through braided cables, created an arc; the resulting plasma was accelerated forward and deposited onto fused silica substrates. The substrates were mounted either on a fixed mounting plate or a flip-up shield directly in front of the plasma gun (right side of fig. 3). During operation, slight electrode deterioration occurred, ranging from discoloration and pitting to small cracks on the inner electrode.

Capacitor Bank

The capacitor bank consisted of fourteen 400 μF discharge capacitors (10 KJ total energy capability) mounted in a double rack cabinet. Also included in the cabinet were the charging circuitry and safety bleed resistors. Vacuum relays were used to switch between charge and discharge cycles, and the high voltage bleed resistors dissipated the bank energy in case of system shutdown. Access to the high voltage components was restricted by 6.4 mm thick polycarbonate shields. Interlock switches were also incorporated throughout the system to provide additional hazard protection. Current from the capacitors was fed to the busbar (described in the next section) through 50Ω triaxial cables encased in plastic-coated flexible conduit. In order to minimize inductance, the two outer conductors of these cables were used.

Busbar

The busbar acted primarily as a termination for the capacitor cables, but also include a voltage reversal-suppressing diode, a current measuring transformer, and a voltage probe. It was enclosed in a box made of 6.4 mm thick polycarbonate (fig. 4). The busbar itself consisted essentially of two 6.4 mm thick rectangular copper plates. The current transformer was sandwiched between the plates with layers of epoxy insulation, while the voltage probe was mounted outside the busbar. Bolts were used to connect the two plates together. Since high repulsive forces between the plates were anticipated, precautions were taken to ensure that the busbar was adequately reinforced. Two overhanging 6.4 mm thick insulated steel plates were bolted around the current measuring transformer, and a clamp was used to maintain electrical contact with the diode. Custom machined copper cylinders with rounded shoulders were used as cable terminations; this allowed the cable sheaths to be slipped over and clamped to the cylinder with small hose clamps.

Current from the cables was fed into the belljar through a coaxial feed-thru. The inner conductor of the feed-thru extended from the far busbar plate, through the current probe, to the near plate, and then through the conductor and into the belljar. Specially designed finger clamps were used to attach the conductor rods to the busbar plates to maximize the current-carrying capacity of the rods. Similar clamps were also used at the other end of the feed-thru rods, as well as on the center electrode of the railgun.

Electronic Instrumentation

Measurement of the circuit characteristics of the plasma gun operation was accomplished with the electronics system shown in figure 5. A Tektronix® 7854 digitizing oscilloscope was used as the recording device. A 1000x-20kV voltage probe mounted on the busbar and connected across the feed-thru was used to monitor the voltage across the gun, and a 0.001 V/A pulse current measuring transformer mounted between the busbar plates was used to monitor the current. The voltage probe was connected to a compensating network, which in turn was plugged into a custom-built junction box which contained a fuseable jumper for the purpose of grounding one side of the high voltage circuit. This prevented the pick-up of spurious noise by the scope. Potential ground-loop problems were avoided by placing the jumper at the scope input.

Current measurements were made by means of the current measuring transformer (connected to an attenuator through an RG/58U coaxial cable). The pulse characteristics of the attenuator were evaluated using the square wave calibration signal from the front panel of the scope, and it was determined that the attenuator contributed negligible distortion to the rise and fall times of the pulse transitions. Statistical evaluation indicated the attenuation to be approximately 2.067x. The attenuator was necessary because of the high output of the current probe due to the high discharge currents, which were typically 100 kA.

The scope was set to trigger on the rising edge of the current waveform. When the discharge occurred, the scope recorded the voltage and current waveforms. Program software previously loaded into the scope (through the

attached Waveform Calculator) then rescaled the waveform to account for the attenuation factor and probe sensitivities, and then multiplied the two to obtain the power waveform. These were then characterized using waveform analysis software on a Tektronix®4052 Graphics Terminal and values of certain parameters of interest, including rise and fall times, pulse widths, 100 percent (peak) values, dissipated energy, stored energy, and the fraction of the initial bank energy dissipated in the belljar were computed and recorded. Finally, a printer unit provided a hard copy of the waveforms. Figure 6 provides an overview of the entire system.

System Operation

Typical plasma gun operation was as follows: the belljar was evacuated (~10^{-6} torr) and the capacitor bank charged to ~1800 V. Once the capacitor bank was charged, the high voltage power supply was disconnected from the bank. A pushbutton switch was then used to apply power to the two solenoids in the belljar, which pulled in the center electrode until contact was made with the outer electrode. This created the arc, and the energy stored in the capacitor was rapidly dissipated, typically within one millisecond. The digitizing oscilloscope recorded the voltage, current, and power waveforms.

Capacitor bank voltages of ~1800 V allowed acceptable deposition rates while minimizing damage resulting from the high peak discharge currents, which for this voltage range were usually 100 kA± 10 percent. At this voltage level, the resulting shock, thermal stresses, Lorentz forces, and carbon deposition on insulating surfaces usually caused enough deterioration of the plasma gun mechanism to limit each run to no more than ten discharges. It was found that deposition rates for this railgun fell off sharply as the voltage was decreased, while increased frequency of dielectric breakdown usually accompanied higher voltage levels.

Film Deposition and Characterization

Typical voltage, current, and power waveforms are shown in figure 7 and parameter values are listed in Table 1. Voltages of ~1800 V gave currents on the order of 100 kA which resulted in power of about 73 MW being dissipated by the gun. One firing event lasted about 0.6 to 0.8 msec.

Several methods were used to characterize the films. These included scanning electron microscopy (SEM), scanning transmission electron microscopy (STEM), X-ray diffraction, X-ray absorption, spectrographic analysis (plasma), energy dispersive spectroscropy (EDS), and selected area electron diffraction (SAED). Optical absorption and electrical resistivity measurements were performed as well.

Several sets of films were deposited on fused silica substrates, with typically 5 to 10 firings per set. The resulting films were dull gray in color and in poor mechanical attachment to the fused silica substrates. The lack of strong bonding to the substrate is typical of film-substrate interfaces where adsorbed gases and surface contaminants have not been removed (by, for example, ion beam cleaning) prior to film deposition. Evidence of intrinsic stress in

the films could be seen because areas of thick deposits showed a higher incidence of spalling.

Figure 8 shows a SEM micrograph of one film sample at two different magnifications taken from a substrate mounted near the center of the target plate. The film was approximately 2000 Å thick (measured with a Tencor Instruments Alpha-Step Profiler). Figure 9 reveals some features of the structure beneath the larger particles. The underlying layer can be characterized as having a wavy, irregular appearance. Figure 10 shows in even clearer detail this underlying layer.

The film shown in figure 11 was deposited on a substrate placed near the edge of the target plate deposition area, and is devoid of the previously observed larger particles. It consists only of the more uniform underlying layer. Stereo views of this picture revealed a layered structure. Also under stereo view, the irregular structure present in the lower right portion of figure 11 appeared as a "flattened volcano," which readily indicates lifting of the underlying layer.

Observations at much higher magnification and resolution were possible with STEM micrographs. Figure 12 shows a film that was deposited during the first set of firings of this experiment. The dark areas are particles, the gray areas are the background material, and the white areas are tears in the film. For the micrograph (fig. 12) the film was actually removed from the substrate (floated). A cross section of this film appears in figure 13. The uneveness of the surface is readily observed. Figure 14 shows a closer view of the embedded particles, which can be seen to be much smaller than the dark areas mentioned in the discussion of figure 12. The particles are randomly dispersed throughout the film.

The structure and composition of these particles was also investigated; one such particle is shown in figure 15. EDS measurements revealed the presence of Mg, Si, Cl, Fe, Cu, Ca, Ag, and Sn. Elemental dot mappings revealed that the distribution of these elements was fairly uniform throughout the particle. A spectrographic analysis of the original carbon electrode material revealed the presence of Al, B, Ca, Cu, Fe, Mg, Pb, Si, and Zn impurities in the electrode itself. Ca, Fe, and Si were present in the greatest abundance, with concentrations of 100 to 300 ppm (concentrations of the others ranged from 10 to 50 ppm). SAED studies yielded a triangular, repeating spot diffraction pattern indicative of a crystalline structure (fig. 16). The pattern suggests that the crystal may be a silicate hydroxide of one or more of the above metals.

The background film was also examined; a close-up view appears in figure 17. Electron diffraction studies gave results as shown in figure 18. The lack of any pattern indicates an amorphous structure (cf. fig. 16).

Electrical and optical measurements gave additional information about the films. Electrical contacts to the films were made with sputtered gold and then silver paint. The measured resistivities averaged 1.2×10^6 ohm·cm. This value is between the >10" ohm·cm values which have been measured for films deposited from a graphite target (ref. 2) and the value of 0.0174 ohm·cm for graphite itself (ref. 12).

Optical absorption studies were performed on several film samples. Optical transmittance, corrected for surface reflection, was measured over the range of photon energies of 0.5 to 3.5 eV. Corresponding values of the absorption coefficient, α, were obtained. Plots of $(\alpha h\nu)^{1/2}$ versus $h\nu$ (ref. 13) were linear (h = Planck's constant and ν = the frequency of the incident radiation), but gave an optical bond gap, Eg. of ~0 (fig. 19). This is indicative of a more three-coordinated (graphite) than four-coordinated (diamond) structure. For comparison, figure 20 shows a similar plot for a sample produced by ion beam sputtering of a carbon target. It can be seen that Eg > 0, indicating the presence of a greater amount of four-coordinated (diamond-like) carbon (ref. 14).

CONCLUSION

Although the plasma gun mechanism could be operated easily, it suffered from recurring problems. The most troublesome difficulty was that the gun could only be fired 5 to 10 times after each refurbishment of the plasma guns's insulting surfaces; continued firing without refurbishment caused arcing at sites other than at the carbon electrodes. Hence, while the design was suitable for laboratory deposition of carbon films, it would not be useful for film deposition on a production scale. Modification of the electrical connections would also be necessary.

The films produced in these experiments were primarily amorphous. There was no evidence of diamond-like carbon. Inclusions and particulates appear to be an inherent feature of this deposition method. Many of the particles were found to be crystalline (as determined by X-ray diffraction analysis), and commonly contained trace impurities. These impurities were found by spectrographic analysis to be present in the graphite electrode material, and hence it was concluded that this was their source.

Electrical resistivity and optical absorption measurements indicated that while the films were highly resistive (~10^6 ohm·cm), the optical band gap was zero, which indicated a more trigonally than tetrahedrally bonded structure.

REFERENCES

1. Aisenberg, S.; and Chabot, R.: Ion-Beam Deposition of Thin Films of Diamondlike Carbon, J. Appl. Phys. vol. 42 June, 1971, pp. 2953-2958.
2. Banks, B. A.; and Rutledge, S. K.: Ion-Beam Sputter Deposited Diamondlike Films. NASA TM-82873, 1982.
3. Holland, L; and Okha, S. M.: Deposition of Hard and Insulating Carbonaceous Films on an r.f. Target in a Butane Plasma. Thin Solid Films vol. 38, 1976, pp. 217-219.
4. Weissmental, C.: Trends in Thin Film Deposition Methods, Proceedings of the 7th International Vacuum Congress and the Third International Conference on Solid Surfaces, R. Dobrozemsky, et al., eds., Vol. II, R. Dobrozemsky et al., 1977, pp. 1533-1544.
5. Michels, C. J.; and Heighway, J. E.; and Johansen, A. E.: Analytical and Experimental Performance of Capacitor Powered Coaxial Plasma Guns. AIAA J. vol. 4 no. 5, May 1966, pp. 823-830.

6. Michels, C. J.: A Resume of Research on Coaxial Plasma Guns Performed at Lewis Research Center. NASA TM X-52431, 1968.
7. Michels, C. J.; and Ramins, P.: Performance of Coaxial Plasma Gun with Various Propellants. Phys. of Fluids Supplement, vol. 7, no. 11, Nov. 1964, pp. 571-574.
8. Posta, S. J.; and Michels, C. J.: 20 kg PFN Capacitor Bank with Solid-State Switching-Pulse Forming Network for Plasma Studies, Rev. Sci. Instrum, vol. 44, Oct. 1973, pp. 1540-1541.
9. Michels, C. J.; and Terdan, F. F.: Characteristics of a 5-Kilojoule, Ignitron-Switched, Fast-Capacitor Bank. NASA TN D-2808, 1965.
10. Sokolowski, M.; et al.: Reactive Pulse Plasma Crystallization of Diamond and Diamond-Like Carbon. J. Cryst. Growth vol. 47, no. 3, Sept. 1979, pp. 421-426.
11. Sokolowski, M.; et al.: The Depositing Thin Films of Materials with High Melting Points on Substrates at Room-Temperature Using the Pulse Plasma Method. Thin Solid Films, vol. 80, 1981, pp. 249-254.
12. Weast, R. C.; ed.: CRC Handbook of Chemistry and Physics 1981-1982 62nd ed. Chemical Rubber Co., 1981.
13. Tauc, J.: Optical Properties of Amorphous Semiconductors. Amorphous and Liquid Semiconductors, J. Tauc, ed., Plenum, 1974, pp. 159-220.
14. Rutledge, S. K.: Unpublished work, 1982.

TABLE 1. - WAVEFORM PARAMETERS FOR FIGURE 7

Voltage waveform	Fully charged voltage	1.768 kV
	Fall time (90 percent to 10 percent)	633 μsec
Current waveform	Peak current	92.84 kA
	Rise time (10 percent to 90 percent)	54.2 μsec
	Fall time	383 μsec
	Pulse width (10 percent level)	499 μsec
Power waveform $\{V(t)\cdot I(t)\}$	Energy stored in capacitor bank	8.755 kJ
	Dissipated energy (integral of power over pulse duration)	6.549 kJ
	Percent energy transferred	74.8 percent

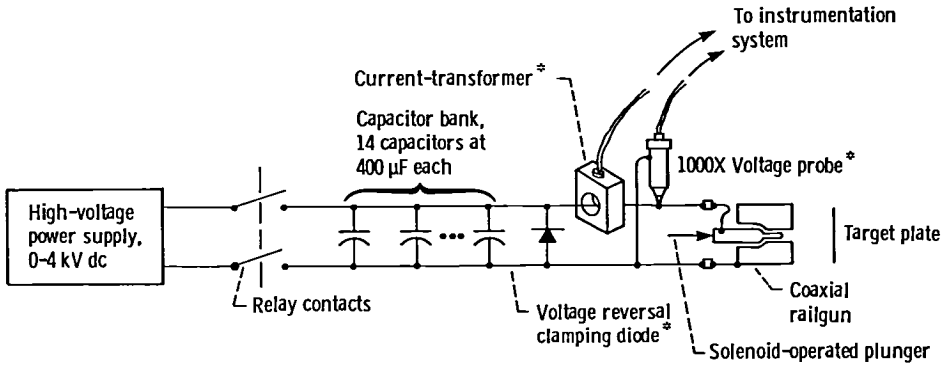

*These components were contained within the busbar assembly, which is not explicitly shown in this schematic.

Figure 1. - Basic elements of plasma gun system.

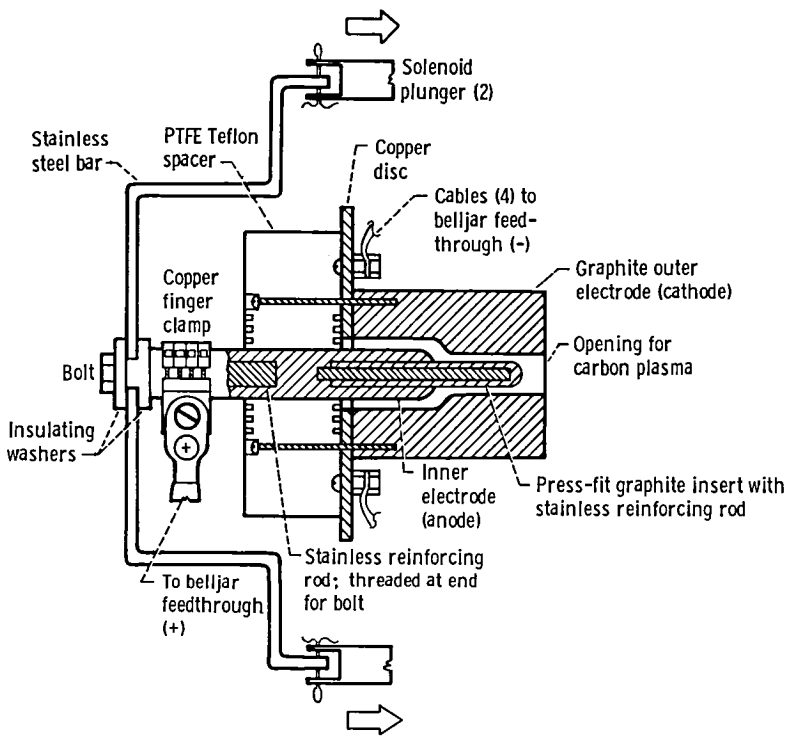

Figure 2. - Schematic representation of the plasma gun mechanism.

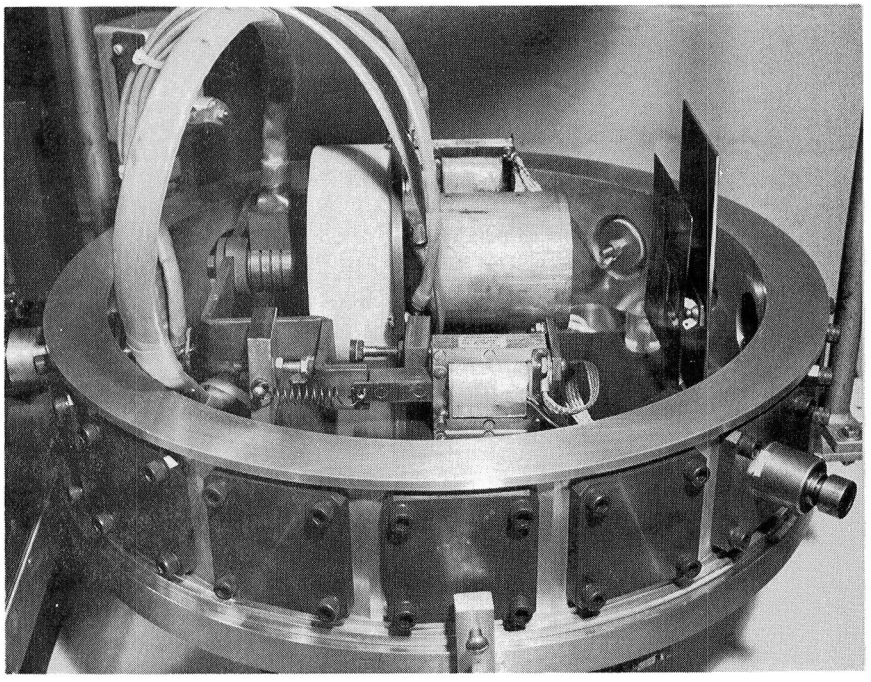

Figure 3. - Close-up view of plasma gun mechanism in base of belljar.

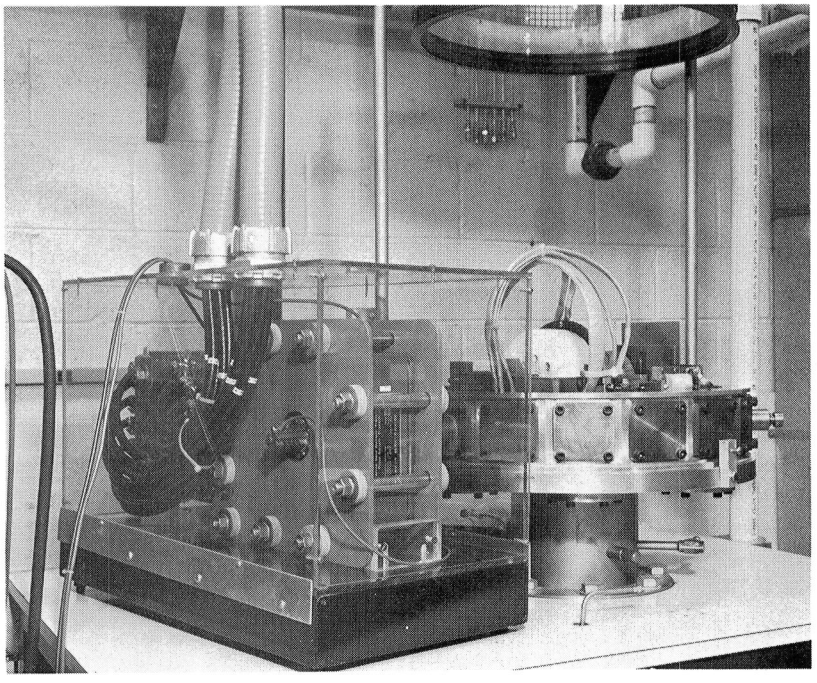

Figure 4. - Close-up of busbar assembly (at left).

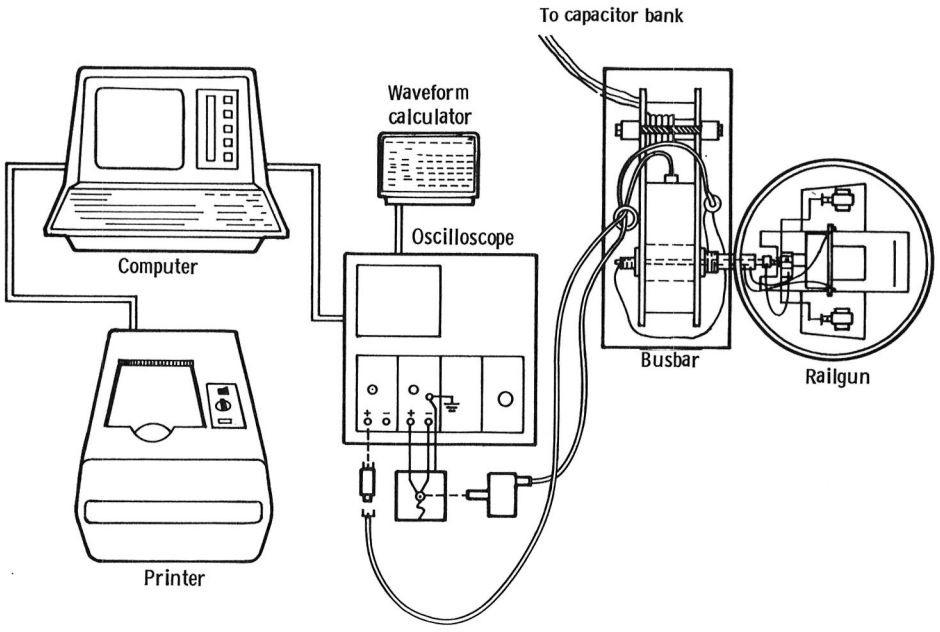

Figure 5. - Diagram of electronics instrumentation and connection to the busbar and plasma gun assemblies.

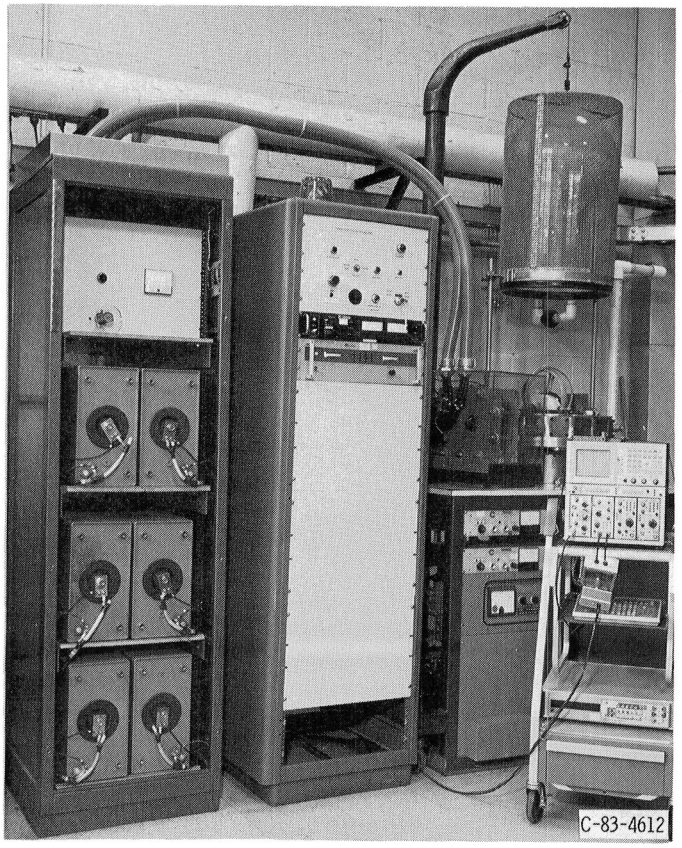

Figure 6. - Left-to-right: Capacitor bank, control panel, busbar, belljar containing the plasma gun, oscilloscope and associated electronics.

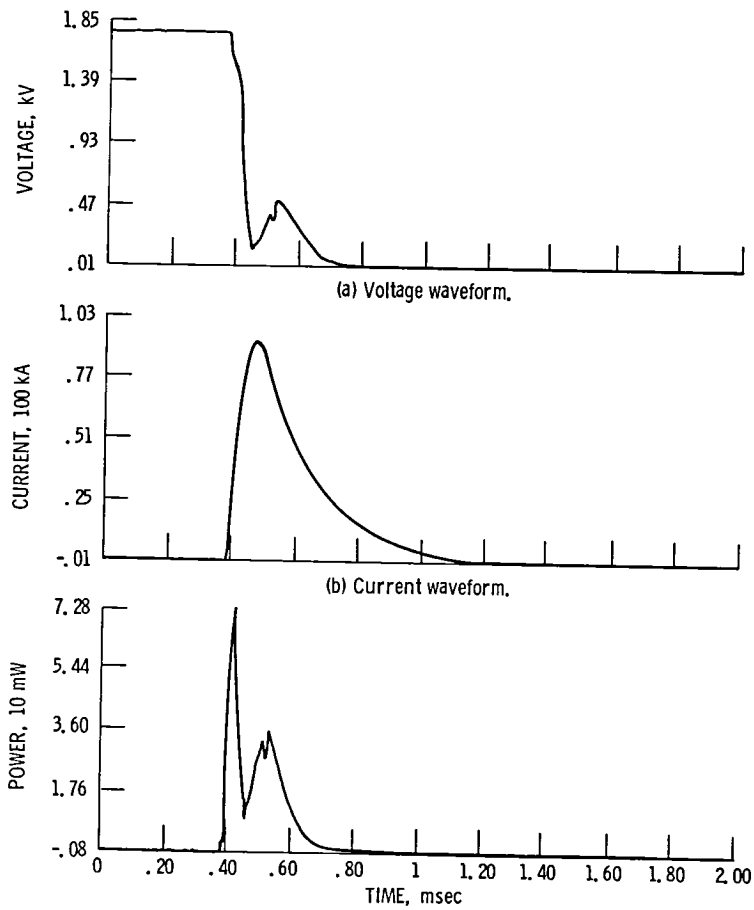

(a) Voltage waveform.

(b) Current waveform.

(c) Power waveform.

Figure 7. - Typical voltage, current, and power waveforms.

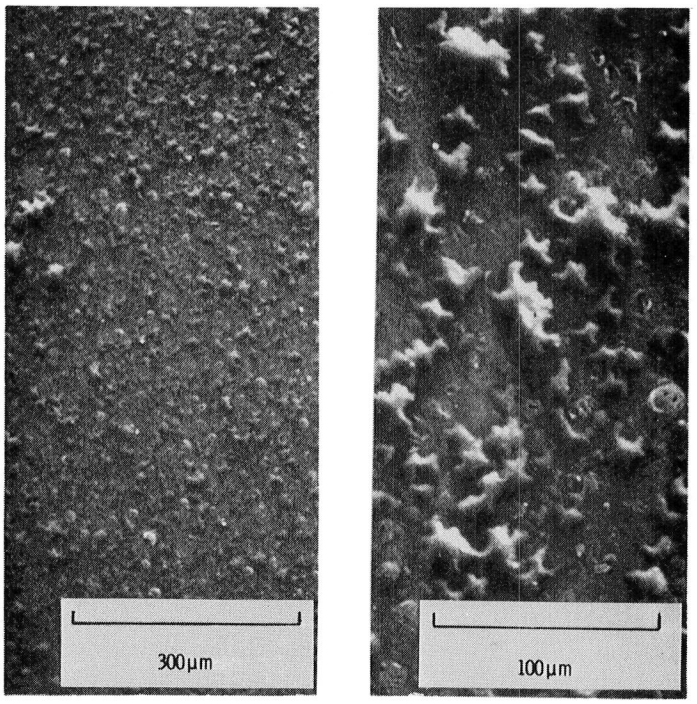

(a) Lower magnification. (b) Higher magnification.

Figure 8. - Scanning electron micrograph of deposited carbon film. Sample taken from center of target area. Thicker areas of the film were spalled.

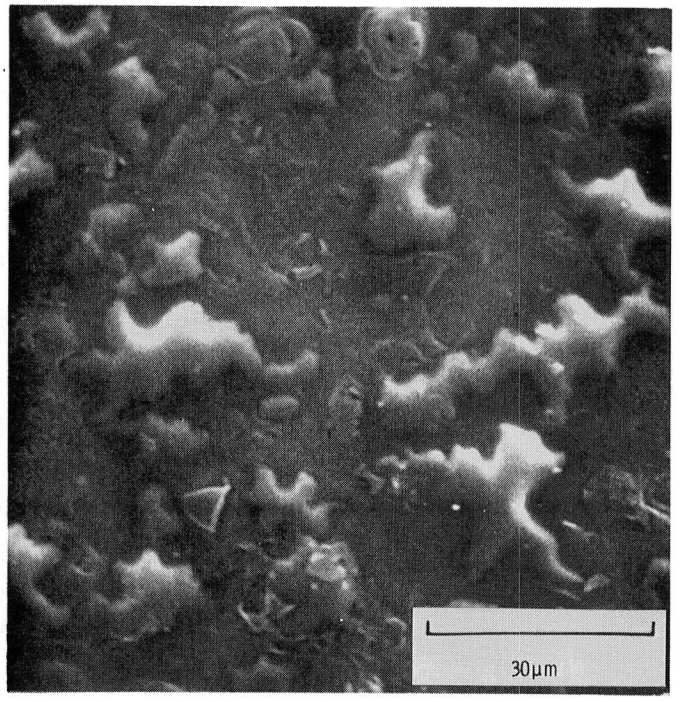

Figure 9. - Film in Figure 8 at increased magnification. Note details of the film beneath the larger deposits. The nonuniform composition is clearly visible at this magnification level.

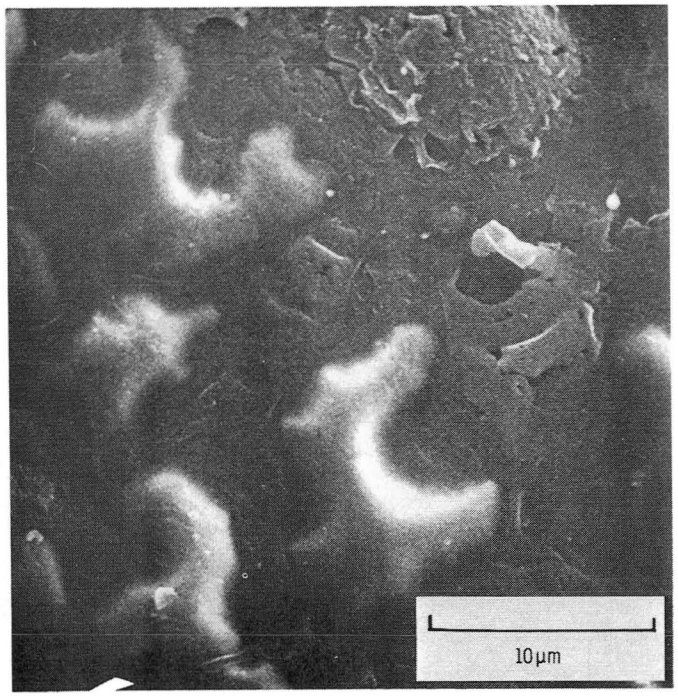

Figure 10. - Film in Figure 8 at very high magnification shows in still greater detail the nonuniformity of the underlying film.

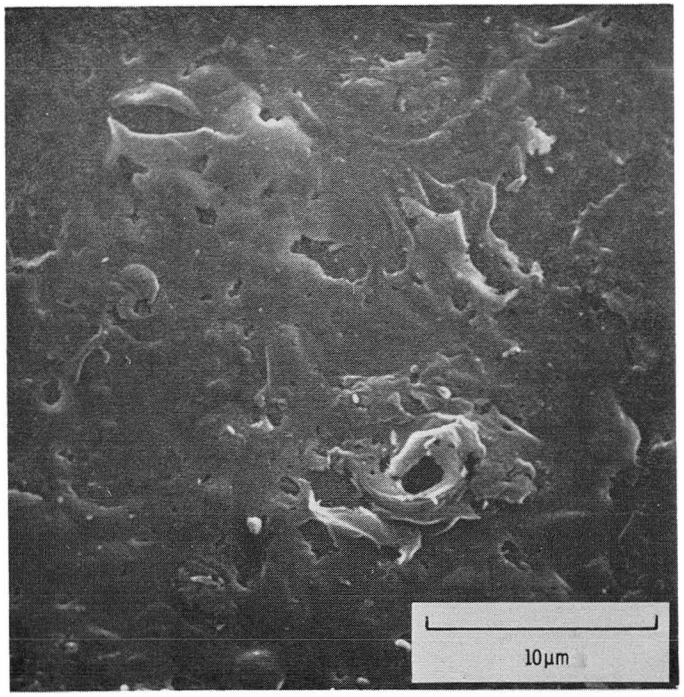

Figure 11. - Scanning electron micrograph of film sample taken from the edge of the target deposition area. Larger features are absent. Lifting and layering of the film can be seen. Feature in lower right has shape of a flattened volcano when viewed stereoscopically.

Figure 12. - Scanning transmission electron micrograph of the film sample shows embedded particles. White areas are tears in the films.

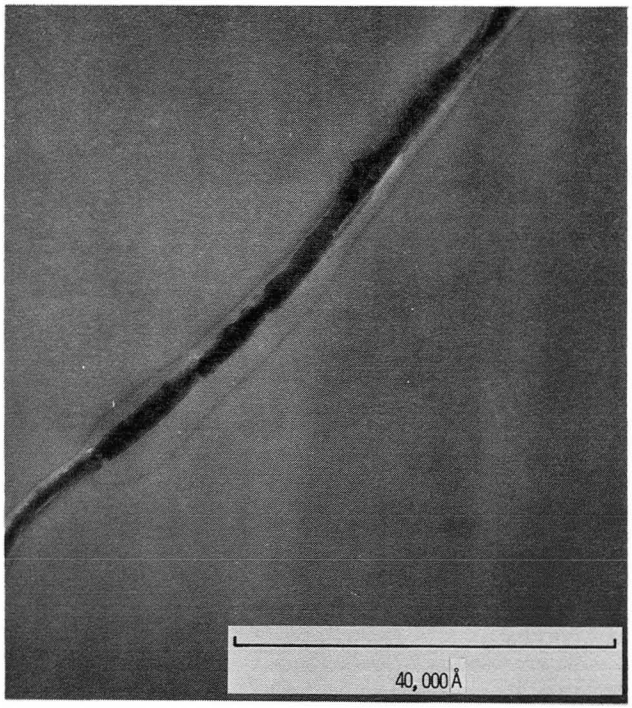

Figure 13. - Cross-sectional view of film sample showing surface irregularity.

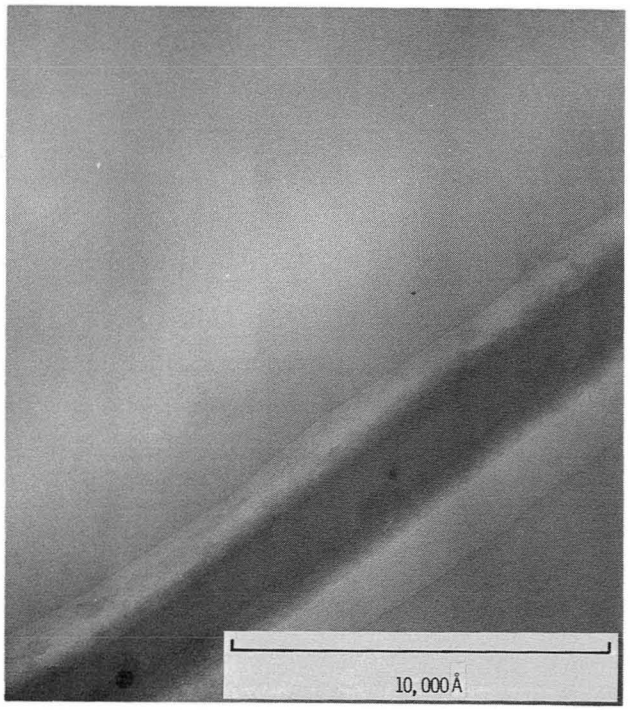

Figure 14. - Cross-sectional view of film sample showing film thickness and random depth of the particles.

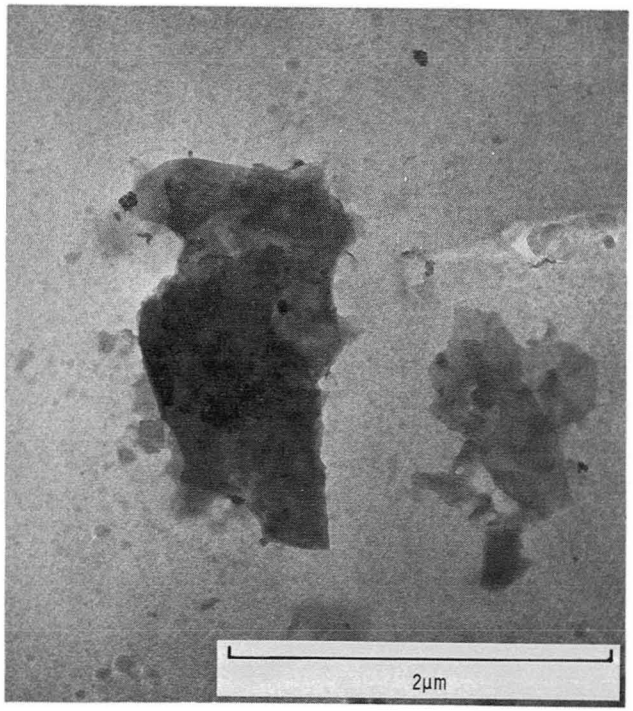

Figure 15. - Typical particle embedded in carbon film.

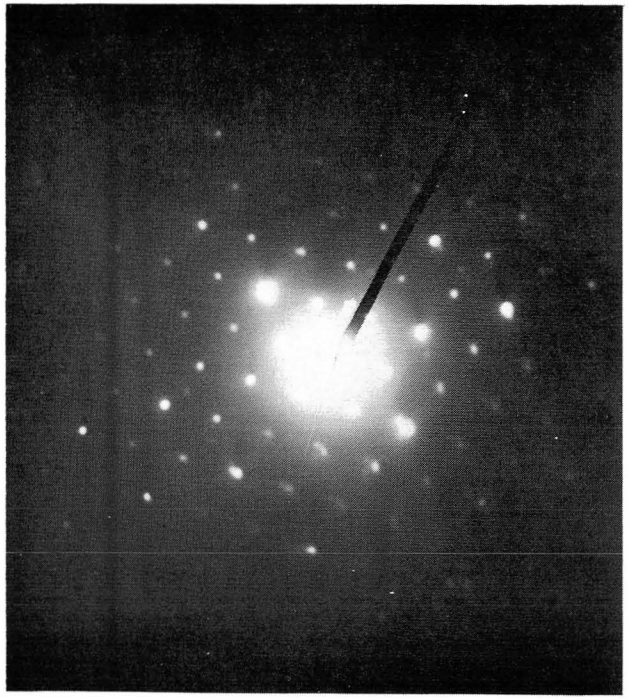

Figure 16. - Selected area electron diffraction pattern for particle in figure 15 indicates presence of a crystalline structure.

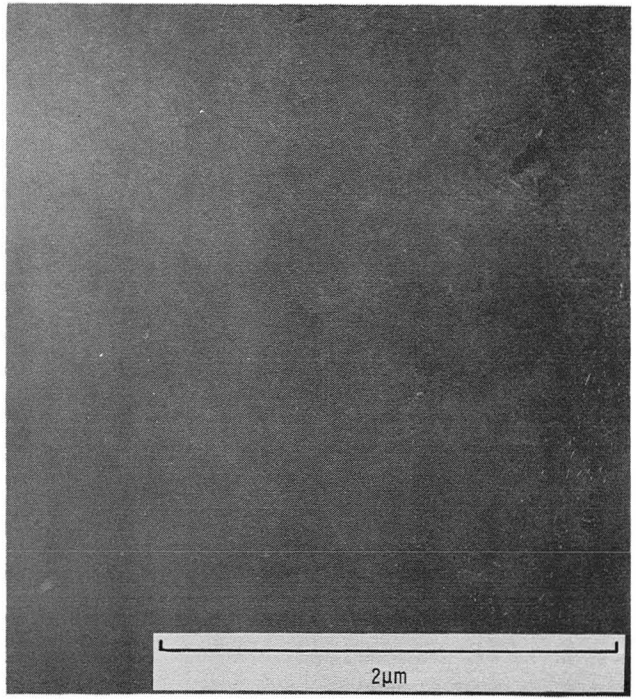

Figure 17. - Micrograph of carbon film background.

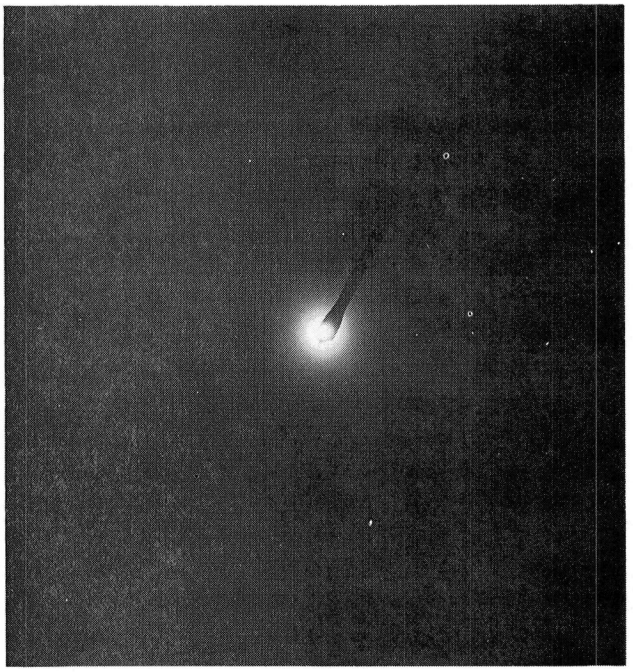

Figure 18. - Electron diffraction study of carbon film background. The lack of any pattern indicates an amorphous structure (cf. Fig. 16).

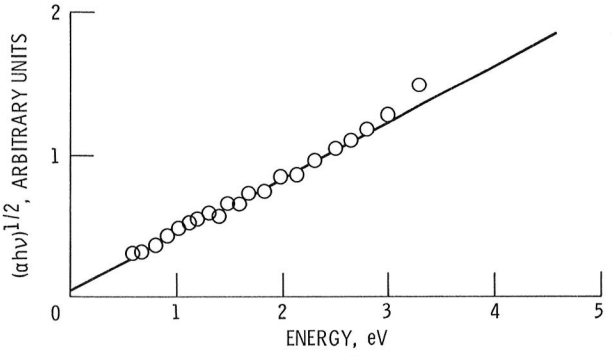

Figure 19. - Plot of $(\alpha h\nu)^{1/2}$ versus $h\nu$ to obtain band gap, Eg, of plasma railgun-deposited sample. Eg $\approx$ 0.

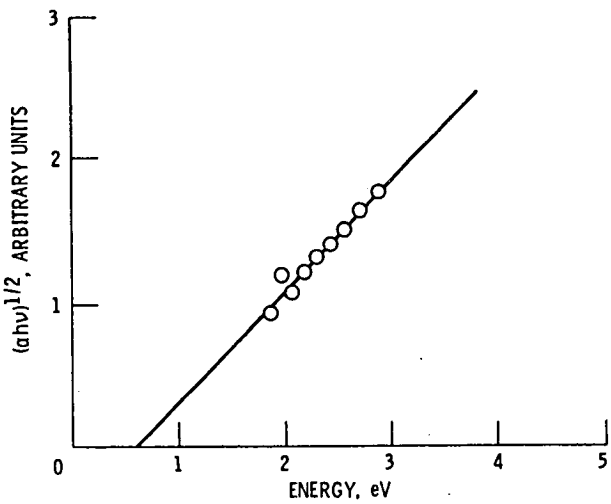

Figure 20. - Plot to obtain Eg of an ion beam sputter-deposited film for comparison with Fig. 19. Eg > 0.

1. Report No.	2. Government Accession No.	3. Recipient's Catalog No.
NASA TM-83600		

4. Title and Subtitle	5. Report Date
Coaxial Carbon Plasma Gun Deposition of Amorphous Carbon Films	March 1984
	6. Performing Organization Code: 506-55-72

7. Author(s)	8. Performing Organization Report No.
Daniel M. Sater, Daniel A. Gulino, and Sharon K. Rutledge	E-2012
	10. Work Unit No.

9. Performing Organization Name and Address	11. Contract or Grant No.
National Aeronautics and Space Administration Lewis Research Center Cleveland, Ohio 44135	
	13. Type of Report and Period Covered: Technical Memorandum

12. Sponsoring Agency Name and Address	14. Sponsoring Agency Code
National Aeronautics and Space Administration Washington, D.C. 20546	

15. Supplementary Notes

Daniel M. Sater, University of Cincinnati, Cincinnati, Ohio; Daniel A. Gulino, NASA Lewis Research Center; Sharon K. Rutledge, Cleveland State University, Cleveland, Ohio.

16. Abstract

A unique plasma gun employing coaxial carbon electrodes has been used in an attempt to deposit thin films of amorphous "diamond-like" carbon. A number of different structural, compositional, and electrical characterization techniques were used to characterize these films. These included scanning electron microscopy, scanning transmission electron microscropy, X-ray diffraction and absorption, spectrographic analysis, energy dispersive spectroscopy, and selected area electron diffraction. Optical absorption and electrical resistivity measurements were also performed. The films were determined to be primarily amorphous, with poor adhesion to fused silica substrates. Many inclusions of particulates were found to be present as well. Analysis of these particulates revealed the presence of trace impurities, such as Fe and Cu, which were also found in the graphite electrode material. Hence it was concluded that the electrodes were the source of these impurities. No evidence of diamond-like crystallite structure was found in any of the film samples. Details of the apparatus, experimental procedure, and film characteristics are presented in this paper.

17. Key Words (Suggested by Author(s))	18. Distribution Statement
Coaxial Plasma Gun Carbon films	Unclassified - unlimited STAR Category 76

19. Security Classif. (of this report)	20. Security Classif. (of this page)	21. No. of pages	22. Price*
Unclassified	Unclassified		

*For sale by the National Technical Information Service, Springfield, Virginia 22161

N84-20404#

National Aeronautics and
Space Administration

Washington, D.C.
20546

Official Business
Penalty for Private Use, $300

SPECIAL FOURTH CLASS MAIL
BOOK

Postage and Fees Paid
National Aeronautics and
Space Administration
NASA-451

NASA

POSTMASTER: If Undeliverable (Section 158
Postal Manual) Do Not Return